PCCP

Cite this: *Phys. Chem. Chem. Phys.*, 2011, **13**, 18069–18077

www.rsc.org/pccp

PAPER

Manganese-Schiff base complexes as catalysts for water photolysis†‡

Gustavo González-Riopedre,[a] M. Isabel Fernández-García,*[a] Ana M. González-Noya,[a] M. Ángeles Vázquez-Fernández,[a] Manuel R. Bermejo[b] and Marcelino Maneiro*[a]

Received 12th April 2011, Accepted 25th August 2011
DOI: 10.1039/c1cp21154d

Four manganese(III)-Schiff base complexes (**1–4**) of formula $[MnL^n(H_2O)_2]_2(ClO_4)_2{\cdot}mH_2O$ (n = 1–4; m = 0, 1) have been prepared. The multidentate H_2L^n Schiff base ligands consist of 3*R*,5*R*-substituted *N*,*N*′-bis(salicylidene)-1,2-diimino-2,2-dimethylethane, where R = OEt, OMe, Br or Cl. The complexes have been thoroughly characterized by elemental analysis, mass spectrometry, magnetic susceptibility measurements, IR, UV, paramagnetic ^{1}H NMR and EPR spectroscopies. Other properties, including redox studies and molar conductivity measurements, have also been assessed. The crystal structure of **1** was solved by X-ray diffraction, which revealed the dimeric nature of the compound through μ-aqua bridges. The ability of these complexes to split water has been studied by water photolysis experiments, with the oxygen evolution measured in aqueous media in the presence of a hydrogen acceptor (*p*-benzoquinone), the reduction of which was followed by UV-spectroscopy. The discussion of the photolytic behaviour includes advances in the knowledge of the structural motifs and the chemical activity of this type of complex, as revealed by the development of several characterization techniques in the last decade. Parallel-mode Mn^{III} EPR shows that complexes **1–4** not only mimic reactivity but also share some structural characteristics from partially assembled natural OEC clusters.

Introduction

The development of a catalyst for the production of oxygen from water is crucial in order to achieve environmentally clean fuel combustion.[1–3] The Oxygen Evolving Complex (OEC) is the native enzyme that catalyses this process in photosynthesis and this is the most efficient system for splitting water catalytically.[4–6] Modelling the OEC with artificial inorganic complexes is a powerful tool for testing different aspects and scientific hypotheses concerning the nature and behaviour of the OEC cluster,[7–14] but this research also represents a way to develop a stable and highly active catalyst for electrochemical and photochemical water oxidation.[15–18]

The vast amount of work that is now being carried out in this field has been covered in the recent review articles listed above. The growing world energy demand, along with the need for control of gas emissions, explains the current relevance of this research, which has not always been supported to the same extent in the last few decades. This idea can be illustrated with an example: over the last decade a number of publications have appeared that were inspired by the $[(bpy)_2Mn^{III}(\mu\text{-}O)_2Mn^{IV}(bpy)_2]^{3+}$ model (see, for instance ref. 19–22), but none of these papers refer back to the original work by Calvin in the seventies, at the time of the first oil crisis, when this model was first proposed for photosynthetic solar energy conversion.[23] However, Calvin's model has inspired scientists for decades; for example, in the eighties, Kaneko *et al.*[24] used this complex for water oxidation with Ce(IV) in a heterogeneous phase by adsorbing it into kaolin clay, in a way that seems to evoke more recent publications. Surprisingly, this paper has barely been cited in the last decade either, probably due to the lack of continuity in research into this area.

On the other hand, a significant part of the scientific community has been fascinated for years by artificial models with very complicated architectures. Simple models did not appear to be valid. The first expiration date of the original Calvin model seemed to be just several months after its proposal[25] but nearly four decades later it is still revisited often. In fact, simple models have afforded some of the best results for water oxidation.[11,15,18,26,27]

McAuliffe and co-workers proved the suitability of the manganese complexes of tetradentate Schiff base ligands (with an N_2O_2 donor set) as catalysts for water photolysis.[28,29] Schiff bases are well-known and economical organic ligands and

[a] *Departamento de Química Inorgánica, Facultade de Ciencias, Universidade de Santiago de Compostela, Avda., Alfonso X, Lugo E-27002, Spain. E-mail: marcelino.maneiro@usc.es; Fax: +34 982285872; Tel: +34 982824106*
[b] *Departamento de Química Inorgánica, Facultade de Química, Universidade de Santiago de Compostela, Santiago de Compostela, E-15782, Spain*

† In memory of the late Professor Charles A. McAuliffe.

‡ Electronic supplementary information (ESI) available: CCDC reference number 821534. For ESI and crystallographic data in CIF or other electronic format see DOI: 10.1039/c1cp21154d

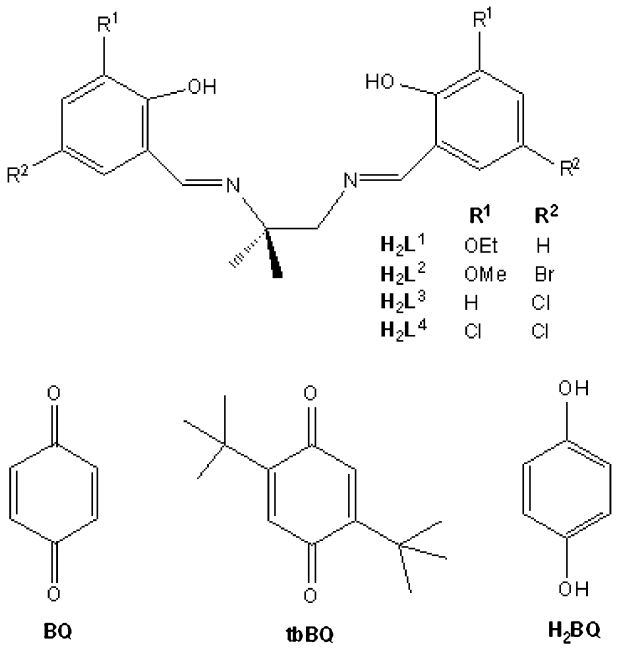

Scheme 1 Representation of the Schiff bases (up) and *p*-benzoquinone (BQ), 2,5-*tert*-butyl-*p*-benzoquinone (tbBQ) and hydroquinone (H_2BQ).

some of them can reproduce the chemistry of the most expensive porphyrins.[2,11] The energetics involved in the formation of the azomethine group and its stability *versus* primary amines would explain why Nature is likely to choose these organic residues instead of other more unfavourable systems. Besides, this type of ligand allows very versatile designs, which are able to modify its basic character or steric properties depending on the nature of the substituents on the aromatic rings.[30] The strong chelate effect provided by these ligands confers an increased robustness on their complexes in comparison to other systems.

Herein we report four novel manganese-Schiff base complexes that are able to coordinate water molecules. The Schiff bases employed are depicted in Scheme 1. The new complexes were found to possess photolytic activity, as measured through the oxygen evolution from these systems in aqueous media. These complexes represent a model based on previous findings in water photolysis[28] and they produce a similar activity. However, in the present work, the discussion concerning the photolytic behaviour encompasses the advances made in recent years, particularly the new insights on the structural features ascertained through the development of characterization techniques, as well as our own experience in manganese-Schiff base systems as catalysts for other manganese-redox-based catalytic processes.[31–33]

Results

The multidentate Schiff bases, H_2L^n (n = 1–4), used in this study readily react with manganese perchlorate, in the presence of sodium hydroxide and air, to give compounds **1–4**. Elemental analysis of the complexes indicated that they have the general stoichiometry $[MnL^n(H_2O)_2]_2(ClO_4)_2{\cdot}mH_2O$, where L signifies the ligand in its dianionic form and m = 0, 1. The analytical, magnetic, spectroscopic and mass spectrometry data are given in the Experimental section.

All of the complexes exhibit room temperature magnetic moments close to the spin only value of 4.9 B.M. expected for a high spin magnetically dilute d^4 manganese(III) ion. Such behaviour is typical for this class of compounds. Previous magnetic studies on related compounds between 300 and 5 K indicated little or no antiferromagnetic interaction between the metal centres.[30,34] The room temperature magnetic moments observed in this study do not give cause to suppose that any different magnetic behaviour should occur. All of the FAB mass spectra show peaks relating to fragments of the form $[MnL]^+$, thus indicating ligand coordination to the metal centre. Furthermore, some complexes exhibit peaks due to the fragment $[Mn_2L_2]^+$, which can be tentatively attributed to the presence of dimeric species in solution (Fig. S1, ESI‡).

All of the complexes show similar IR features, with a strong band observed between 1626–1612 cm^{-1} attributable to $\nu(C{=}N_{imine})$, which is 6–18 cm^{-1} lower than the corresponding band in the free ligand. A shift in the $\nu(C{-}O_{phenol})$ band to a higher frequency (6–9 cm^{-1}) is also observed (Fig. S2, ESI‡). These data suggest the coordination of the Schiff base in its dianionic form to the metal through the inner phenol oxygen and the imine nitrogen atoms. The IR spectra also show broad unsplit bands at *ca.* 1120 cm^{-1} along with bands at 630 cm^{-1}, which is indicative of the presence of the uncoordinated perchlorate anion. The presence of a broad band at about 3400 cm^{-1} is associated with coordinated and/or solvated water molecules.

The electronic spectroscopic data are very similar for compounds **1–4**, indicating that the Mn(III) complexes behave as high-spin octahedral d^4 systems that probably suffer a significant Jahn–Teller distortion, which affects the spectra and complicates their interpretation (Fig. 1). A broad shoulder at around 540–600 nm (ε = 120–500 M^{-1} cm^{-1}) is attributable to a d–d transition, while it is reasonable to assign the broad band at 440–480 nm (ε = 2400–3100 M^{-1} cm^{-1}) to the phenolate → Mn(III) charge-transfer. The peak at around 330 nm (ε = 7000–10000 M^{-1} cm^{-1}) can be assigned to an intraligand π–π* transition. The energy and intensity of the LMCT and d–d transitions are consistent with those reported for related Mn^{III} complexes.[35,36]

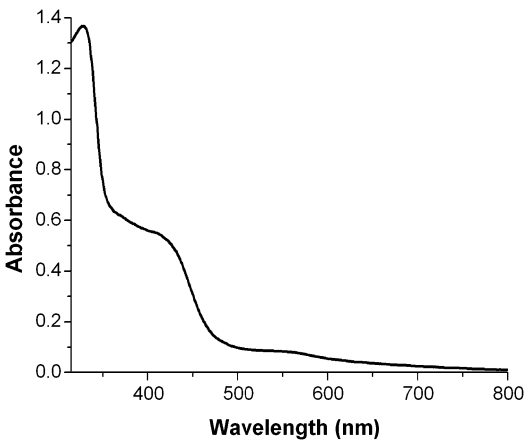

Fig. 1 UV spectrum (in methanol) of **1** (2×10^{-4} M).

Paramagnetic ^{1}H NMR studies of the complexes serve to substantiate the formation of the manganese(III) complexes.[31,37–39] The spectra contain between two and three upfield proton resonances, outside the diamagnetic region (δ = 0–14 ppm) and these are due to the isotropically shifting ligand protons for high-spin manganese(III) complexes in an octahedral field. The signals must arise from the H4 and H5 protons of the aromatic phenoxy rings. The signals between −20.73 and −30.52 ppm are due to the H4 protons, while the resonances from −15.70 to −21.50 ppm are due to H5 protons. The signal corresponding to the H5 protons appears to be split into a doublet owing to the asymmetric nature of the Schiff base ligand in these complexes (Fig. S3, ESI‡).[35]

The electrochemical behaviour of complexes **1–4** with both reduction and oxidation waves can be defined as quasi-reversible as their peak to peak separation varies with the scan rate (a slower scan rate gives rise to more reversible character). Normal pulse voltammetry can be applied to such systems and provides an additional proof of the oxidation state of the manganese in the former complexes. Anodic and cathodic currents were observed when the initial potentials were more negative than the wave range. However, when the initial potentials were more positive than the wave voltage range, only cathodic currents were observed (Fig. 2). These data indicate that in solution only the oxidised forms of the redox systems exist, *i.e.* manganese(III).

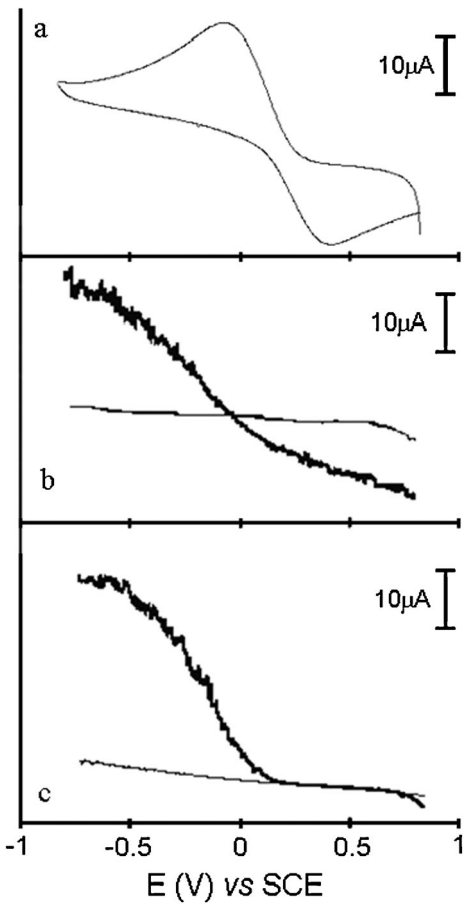

Fig. 2 (a) Cyclic voltammogram for **4** at a scan rate of 0.05 V s^{-1}; (b) normal pulse voltammogram (NPV) for **4** using an anodic scan; (c) NPV for **4** using a cathodic scan.

Crystal structure of 1

Recrystallisation of $[MnL^1(H_2O)_2]_2(ClO_4)_2$ (**1**) from methanol by slow evaporation afforded reddish-brown crystals from which we determined the molecular structure. A stick view of **1** is shown in Fig. 3. The main bond lengths and angles are listed in Table 1. Experimental details are given in Table S1 (ESI‡).

The crystallographic data show that the geometry around the manganese ion is distorted octahedral. The coordination sphere around each manganese centre comprises the planar Schiff base ligand, which is tightly bound to the metal ion through the inner N_2O_2 compartment by the N_{imine} and O_{phenol} atoms. The equatorial Mn–N_{imine} (1.976–1.986 Å) and Mn–O_{phenol} (1.873–1.882 Å) bond lengths are typical of such complexes[33,38] and corroborate the bisdeprotonation of the ligands.

The coordination sphere around each manganese centre is completed by capping water molecules. The Mn–O_{water} distances of 2.254 and 2.271 Å are considerably longer than the equatorial Mn–O bond lengths quoted above, indicating that the Jahn–Teller elongation expected for a high-spin d^4 manganese(III) ion is present in these complexes. The deviation from an ideal octahedral geometry is also revealed by the range of angles observed around the metal centre (from 82.8° to 93.54°), as well as by the interaxial OW–Mn–OW

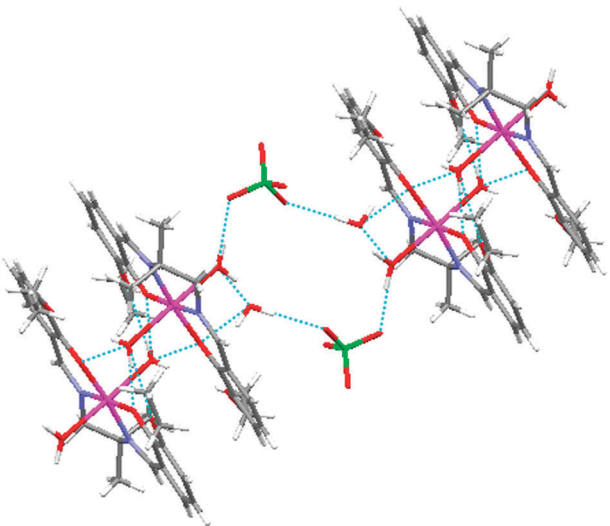

Fig. 3 Stick diagram for **1** showing the hydrogen bonding between adjacent $[MnL^1(H_2O)_2]_2^{2+}$ dimeric units through perchlorate anions and water lattice molecules.

Table 1 Selected bond lengths (Å) and angles (°) for **1**

Mn1–N8	1.986(5)	Mn1–O27	2.254(5)
Mn1–N11	1.976(5)	Mn1–O28	2.271(5)
Mn1–O19	1.882(4)	C7–N8	1.300(7)
Mn1–O21	1.873(4)	C12–N11	1.275(8)
O21–Mn1–O19	93.54(15)	O19–Mn1–O27	87.26(17)
O21–Mn1–N11	92.96(17)	N11–Mn1–O27	89.6(2)
O19–Mn1–N11	172.82(18)	N8–Mn1–O27	89.8(2)
O21–Mn1–N8	175.71(18)	O21–Mn1–O28	89.36(17)
O19–Mn1–N8	90.75(18)	O19–Mn1–O28	91.23(18)
N11–Mn1–N8	82.8(2)	N11–Mn1–O28	91.91(19)
O21–Mn1–O27	90.37(18)	N8–Mn1–O28	90.61(19)
O27–Mn1–O28	178.45(16)		

angle of 178.45°. The perchlorate anion constitutes the second coordination sphere.

The superstructure of the complexes involves associations through a combination of π-aryl interactions and hydrogen bonds between capping water and outer phenoxy and axial water oxygen atoms of the neighbouring Schiff base ligand. The distances and angles involving hydrogen bonding are shown in Table S2 (ESI‡). The oxygen atom of an axial water molecule O(28) establishes a hydrogen bond with O(20) and O(22) of the ethoxy groups and with O(19) and O(21) of the phenoxy group of the ligand of the neighbouring complex, thus acting as μ-aquo bridges. The dimeric units are also stabilized through π-stacking interactions between the aromatic rings. This results in Mn···Mn distances of about 4.917 Å, which are considerably shorter than 10 Å for monomeric compounds,[40] but they are longer than those in other complexes with μ-phenoxo bridges.[30] These types of $[MnL(H_2O)_2]_2^{2+}$ systems have previously been reported[31,33] as μ-aqua dimers. However, these Mn···Mn distances are too long to establish intermetallic interactions between neighbouring manganese ions, a situation in accordance with the non-antiferromagnetic behaviour shown by the magnetic studies.

Moreover, the μ-aqua dimers are interconnected by hydrogen bonds involving the perchlorate counterions. In this way, pairs of neighbouring μ-aquo dimers are linked by two perchlorate anions. This hydrogen bonding scheme arises from the interactions of two perchlorate ions, which establish two pairs of hydrogen bonds to two adjacent μ-aquo dimers.

EPR spectroscopy

Parallel-mode EPR (microwave field H_1 is parallel to the static field H_0) enables one-electron $\Delta M_S = 0$ transitions to be detected that are hardly observable with a conventional EPR method ($H_1 \perp H_0$, perpendicular mode). Mn^{3+} has an integer electron spin, $S = 2$, and has been shown for powdered samples to develop a characteristic sextet pattern in parallel-mode EPR.[41] The sextet is centred at around $g_{eff} = 8$ and is split by a hyperfine interaction $A = 44$–55 G due to the Mn nucleus ($I = 5/2$). A similar sextet is also detectable by perpendicular-mode EPR but the signal intensity is significantly weaker and the peak resolution is worse.

The parallel-mode EPR spectrum of **1** is shown in Fig. 4. Only the low-field portion of the spectrum is shown, since additional lines were not detected at higher fields. The centre position of the sextet ($g_{eff} = 8.09$) and hyperfine splitting ($A_{||} = 44$ G) are identical for all of the complexes and are close to those previously reported for similar compounds.[32,42]

Water photolysis experiments

The course of the water photolysis experiments was followed in two ways: quantitative oxygen evolved and variation of the electronic spectrum of the quinone during photolysis. The experimental setup was improved with respect to the original experiments by McAuliffe and co-workers[28,29] in order to obtain better sealing of the system (Fig. S4, ESI‡). The use of a methacrylate bath allows magnetic stirring and avoids the use of a mechanical stirrer, since this latter option has a detrimental effect on the reproducibility of the dissolved oxygen measurements. On the other hand, the use of a flow cell enhances the airtight nature of the experimental setup for the withdrawal of aliquots for UV monitoring.

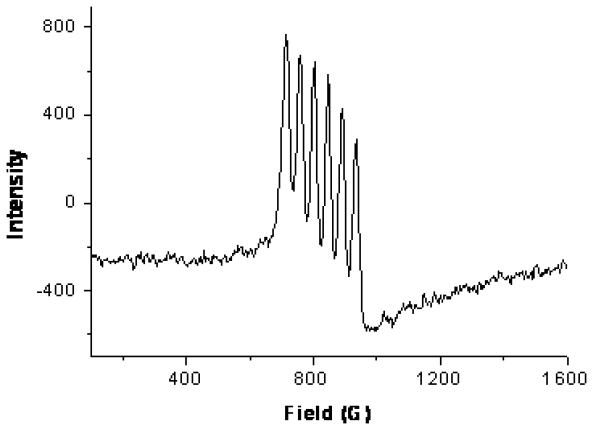

Fig. 4 Parallel-mode EPR of **1** in toluene:dmf:EtOH (2 : 1:drop) solution. Conditions: frequency, 9.37 GHz; $T = 9$ K; 20 mW microwave power.

The reduction of *p*-benzoquinone (BQ) to hydroquinone (H_2BQ) can be easily followed by UV spectroscopy (Fig. S5, ESI‡). BQ in water has a major absorption at 246 nm ($\varepsilon = 2.2 \times 10^4$ M^{-1} cm^{-1}), which decreased during the experiments, whilst a characteristic hydroquinone peak at 290 nm developed (Fig. S6, ESI‡). Photolysis of an aqueous solution containing only BQ leads to a slow decrease in the amount of BQ and to the formation of a mixture of H_2BQ and 2-hydroxy-*p*-benzoquinone[43] without the generation of molecular oxygen.

The time courses of oxygen evolution on irradiating solutions of complexes **1–4** containing BQ are shown in Fig. 5. Oxygen was not evolved in the absence of BQ in the present studies. The use of 2,5-*tert*-butyl-*p*-benzoquinone (tbBQ) instead of BQ did not generate dioxygen either.

The concentration of dioxygen in the solutions during the experiments increased linearly during irradiation, but when the light was switched off the evolution of dioxygen into the solution fell sharply; on starting irradiation once more the dioxygen evolution rate returned to the level originally observed (Fig. S7, ESI‡).

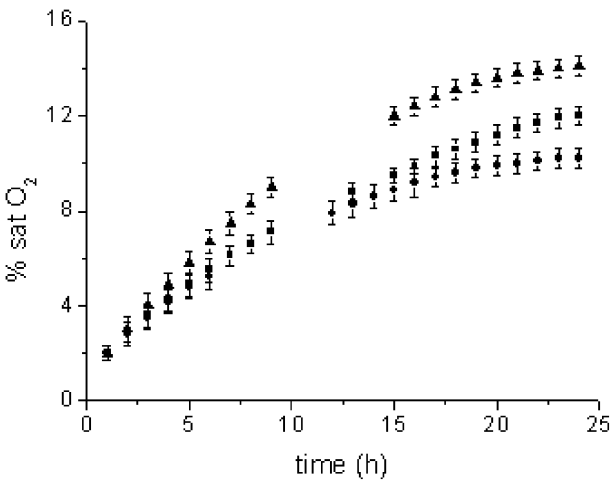

Fig. 5 Plot of percentage O_2 dissolved in solution *vs.* time for complexes **1** (◆), **3** (■) and **4** (▲).

Discussion

Structural studies in solution

An initial discussion point for the catalytic behaviour of these compounds concerns the original structure of **1–4** in solution. Some authors proposed for similar compounds that the dimeric structure found in the solid state by X-ray crystallography is not preserved in solution.[44] This point could be supported, for instance, by molar conductivity measurements for the complexes (in the range 85–97 μS for the complexes reported here), which are consistent with the presence of 1 : 1 electrolytes.[45] Nevertheless, these measurements were carried out on samples in the coordinating solvent DMF, and this solvent could interfere significantly in the structure of these complexes since the lability (and solvent exchange) of the axial positions is a well known phenomenon for this type of compound.[46] In fact, other techniques suggest that the μ-aqua dimeric structures are retained in solution, *e.g.* the dimeric peaks found by FAB mass spectrometry using *meta*-nitrobenzyl alcohol as a liquid matrix, or the band observed in the electronic spectra in water at about 550–600 nm, which is associated with the existence of these dimers in solution.[47]

Moreover, a dimeric nature in solution is also suggested by electrochemical studies. Logarithmic calculations above the limit current of the quasi-reversible wave in the normal pulse voltammogram have been reported for monomeric Mn(III) complexes[48] comparable to the compounds presented here. The results show that a one-electron process is responsible for this wave, which can be written as $[Mn^{III}] \rightarrow [Mn^{II}]$. However, the same treatment applied to the quasi-reversible processes of **1–4** provides a number of electrons close to two (as the rate of reversibility decreases the result of the logarithmical treatment should be interpreted with caution). A two electron oxidation is not expected for monomeric complexes, but two one-electron redox processes $[Mn^{III}, Mn^{III}] \rightarrow [Mn^{II}, Mn^{II}]$ from dimeric species can explain these redox waves. The previously reported monomeric compounds and the present complexes were all measured under the same conditions with approximately equal numbers of moles of manganese. However, the current intensity of the peaks is different. This intensity obeys the Randles–Sevcik equation[49] and all factors in this equation are similar for all of the complexes, except for the diffusion coefficient of each. We found that complexes formulated as monomeric species exhibit higher current intensities in their redox waves than **1–4**. This behaviour is attributed to the monomeric nature of the first type of complex and this gives rise to a higher diffusion coefficient than for **1–4**, which probably have a dimeric structure in solution.

We also carried out peroxidase activity tests with **1–4** and found significant activity using ABTS [2,2′-azinobis(3-ethylbenzothiazoline)-6-sulfonic acid diammonium salt] as a water-soluble trap. The oxidation of the hydroperoxide to generate dioxygen in the peroxidase experiments involves an intramolecular two-electron transfer reaction that is forbidden for monomeric Mn(III) complexes.[31] We conclude that **1–4** should preserve their dimeric structure in solution, either completely or to a significant extent.

The coordination environment around the metal ion is also a relevant feature for catalysis. Parallel-mode EPR has proven to be a powerful tool to investigate integer-spin paramagnetic species such as Mn^{3+}. The spectra of this metal ion are interpreted taking into account that the zero-field splitting (ZFS) dominates the spin Hamiltonian of Mn^{3+}. ZFS was reported to be about $D \approx 3.4$–5.0 cm^{-1} for Mn^{3+} in tetragonal complexes, while the electron Zeeman interaction in X-band EPR magnetic fields is an order of magnitude smaller, 0.2–0.3 cm^{-1}, and the Mn hyperfine term is $\sim$0.1 cm^{-1}.[50–52]

The case where $S = 2$ in strong ZFS has been considered in detail, and the expressions for the energy levels have been derived to the second order in perturbation theory. Strong ZFS splits the spin levels into two non-Kramer (NK) doublets, nominally $M_S = \pm 1$ and $M_S = \pm 2$ states, and a singlet $M_S = 0$ state. The splitting between the doublets and the singlet is large in comparison to the X-band EPR microwave quantum and, therefore, inter-doublet and singlet-to-doublet transitions are *not* allowed. The only transitions allowed are those between the levels within each NK doublet. With the magnetic field oriented along the principal axis of the ZFS tensor ($D \parallel H_0$), these transitions are centred at[53]

$$g_{\mathrm{eff}(1)} = 2g_{\parallel}\left[1 + \frac{36E^2}{(h\nu_0)^2 - 36E^2}\right]^{1/2} \quad (1)$$

$$g_{\mathrm{eff}(2)} = 4g_{\parallel}\left[1 + \frac{(3E^2/D)^2}{(h\nu_0)^2 - (3E^2/D)^2}\right]^{1/2} \quad (2)$$

for the $M_S = \pm 1$ and $M_S = \pm 2$ NK doublets, respectively. The transitions $g_{\mathrm{eff}(1)}$ or $g_{\mathrm{eff}(2)}$ can only be observed using parallel-mode EPR and even then only if the splitting between the levels in the respective doublet at zero field, $6E$ or $3E^2/D$, does not exceed the microwave quantum, $h\nu_0$. In the case of negligible E ($h\nu_0 \gg 6E$ and $3E^2/D$), the transitions are centred exactly at $g_{\mathrm{eff}(1)} = 2g_{\parallel} \approx 4.0$ and at $g_{\mathrm{eff}(1)} = 4g_{\parallel} \approx 8.0$. In frozen solutions, Mn^{3+} complexes are present with many different orientations of the ZFS tensor relative to the magnetic field direction. Each orientation resonates at different g_{eff}, which results in a field-extended "powder" EPR spectrum. In practice, however, only the resonances of eqn (1) for the complexes with $D \| H_0$ are sharp and observable in the powder spectrum.

The signal of **1–4** at $g_{\mathrm{eff}} = 8.09$ should be assigned to $g_{\mathrm{eff}(2)}$. Using eqn (1) and assuming typical values of $D \approx 3.4$–5.0 cm^{-1} and $g_{\parallel} = 1.99$,[54] a value of $E = 0.25$–0.31 cm^{-1} can be estimated ($h\nu_0 = 0.31$ cm^{-1} corresponds to $\nu_0 = 9.37$ GHz in our experiments). Thus, significant rhombic splitting within the $M_S = \pm 1$ NK doublet ($6E = 1.5$–1.8 cm^{-1}) explains the absence of the second $g_{\mathrm{eff}(1)}$ transition in the spectra. The $E/D = 0.05$–0.09 is indicative of ZFS rhombicity in frozen solutions. Slight rhombicity has also been observed for substitutional Mn^{3+} in a rutile single crystal ($E/D = 0.04$)[55] and Mn^{3+}(dibenzoylmethane)$_3$ in polycrystalline powder ($E/D = 0.06$).[54] In the latter two cases, Mn^{3+} has an approximately tetragonal coordination, with two axial O ligands that are slightly more distant than the four equatorial O ligands.

On the other hand, the small[55] Mn hyperfine coupling of 43–44 G in **1–4** is also indicative of the electronic ground state $^5B_{1g}$ (the "hole" residing in the d_{x2-y2} orbital), and thus these compounds are either five-coordinated distorted square-pyramidal complexes or six-coordinated distorted tetragonally

elongated complexes,[56] with two axial O atoms from coordinated water molecules and two O and two N atoms from a tetradentate Schiff base ligand that is equatorially coordinated to the ion.

Photolytic studies

Light absorption at 425 nm in aqueous solution causes a $\pi^* \leftarrow n$ transition and this is responsible for the H abstraction from H_2O by optically excited BQ (BQ*). For BQ in the ground state, an endothermic reaction, uphill by 1.6 eV, was found for the first H abstraction. A stability gain of 1.5 eV occurred for this process when BQ had an electron promoted from an oxygen lone-pair orbital to a ring π^* orbital. The hole site has the ability to abstract a hydrogen atom from water to form a semiquinone without the energetic expense of promoting an electron to the ring π^* orbital, as must occur for ground state BQ.[47]

Awad and Anderson carried out a quantum chemical study on the photogeneration of O_2 from H_2O coordinated to Mn^{III}-Schiff base complexes in the presence of BQ.[47] They concluded that H_2O bonded to Mn^{III} as bridges in the Mn^{III} dimer (an identical model to the structure of **1** reported here; **I** in Scheme 2) starts off the reaction sequence by transferring a hydrogen atom to an O^- created by a $\pi^* \leftarrow n$ optical excitation in BQ (see Fig. S8, ESI‡). This process oxidizes Mn^{III} to Mn^{IV} and creates tightly bound OH^- groups that are polarized sufficiently for easy deprotonation. It is the formation of the strong Mn–OH bond that prevents the formation of 2-hydroxy-*p*-benzoquinone, as it occurs in aqueous solution in the absence of the active Mn complexes. More recently, catalytic studies on olefin epoxidation using this type of complex also revealed the possibility of hydrogen abstraction by Mn^{IV} complexes with terminal hydroxo ligands.[57]

A precipitate was not observed during or after the irradiation experiments catalysed by **1–4**. McAuliffe *et al.* initially suggested the formation of $[Mn^{III}L]_2O$ (where L is the Schiff base) at the end of their experiments, although they subsequently proposed a μ-phenoxy-bridged manganese(III) dimer as the final product (**II** in Scheme 2).[28] This latter arrangement for Mn^{III}-Schiff base complexes was almost unknown when McAuliffe and co-workers reported their first irradiation experiments but μ-phenoxy-bridged manganese(III) dimers subsequently became quite common dispositions found by X-ray crystallography.[30,42,58]

On the basis of the different studies carried out on this type of water photolysis experiment, we propose the overall reaction depicted in Scheme 2 –as suggested previously by McAuliffe and us[28] in a previous tentative mechanism– in an attempt to explain our findings. There is strong evidence for successive hydrogen abstractions from water molecules coordinated to the metal ion by optically excited BQ (BQ*), but uncertainty remains about the manganese complex intermediates formed during this process. We have suggested that the activation state would be a transient dioxygen-bridged manganese complex, which would almost instantaneously decompose to produce dioxygen and a μ-phenoxy-bridged manganese(III) dimer. Recently, μ_2-oxo-bridged manganese dimers have been crystallographically solved[59] and this supports the feasibility of our proposal.

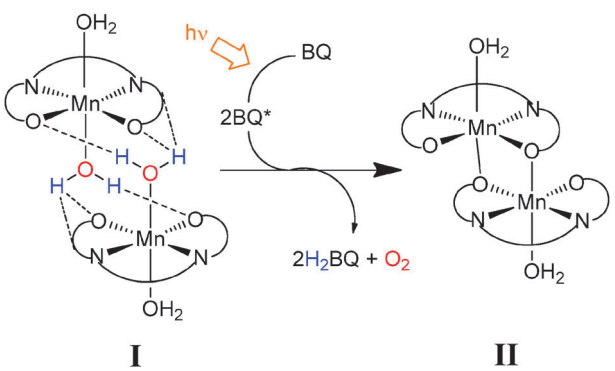

Scheme 2

The fact that dioxygen is not evolved when tbBQ is used instead of BQ indicates a steric requirement in the hydrogen abstraction process. BQ is probably able to enter into the coordination cleft of the μ-aquo dimers, a situation that is not possible for the sterically hindered quinone (Fig. 6). This observation further supports the existence of aqua-bridged dimers in solution.

Our studies with this type of model did not aim to reproduce the structural features of the native OEC. However, it is noteworthy that the EPR characteristics of complexes **1–4** (g_{eff} = 8.1 and $A_{||}$ = 44 G) are almost identical to those reported (g_{eff} = 8.2 and $A_{||}$ = 44 G) for Mn^{III} bound at the high-affinity Mn site in photosystem II (corresponding to the first intermediate of the Mn_4 cluster photo-assembly in PSII).[56] This indicates that the complexes reported here have a ligand coordination structure similar to Mn^{III} in PSII, particularly a six-coordinate distorted tetragonally elongated structure or a five-coordinate distorted square-pyramidal structure.

The rate of tetragonal elongation is also evidenced in the solid state by X-ray crystallography. If we consider the rhombicity factor as the ratio between the manganese-axial oxygen distances and the manganese-equatorial oxygen distances of two dozen or so reported complexes of this type, we calculated values ranging from 1.159 to 1.27. The steric hindrance of the Schiff base is decisive in modulating this rhombicity. We also found a correlation between the peroxidase activity and the rhombicity factor.[31] The peroxidase activity is favoured by a higher Mn–O_{axial} distance since the latter is indicative of a labile ligand that can exchange with the H_2O_2 substrate. In the case of the photolytic activity the H_2O is already coordinated to the manganese ion, but the

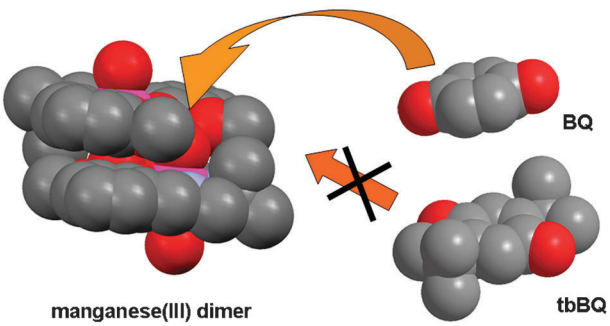

Fig. 6 Spacefilling diagrams of the manganese(III) dimer, BQ and tbBQ, showing the feasible approach of BQ to the coordination cleft. The μ-aqua-bridges are in a cleft with one hydrogen pointing outwards from each side of the dimer.

rhombicity should probably be taken into account for subsequent steps in the reaction, such as the feasible Mn^{IV}–OH intermediates and their subsequent reactions.

Another factor that can be modulated by the choice of a suitable Schiff base is the rate of reversibility in the electrochemical processes of the complexes. The electron-donating or -withdrawing character of the substituents in the phenyl rings induces stabilization of a particular oxidation state for manganese and/or a variation in the redox reversibility of the complex.[32]

Control of all these variables in the design of new compounds inspired by this type of complex is the key issue to achieve more efficient water photolysis systems. The control of the reconstitution of the μ-aqua dimers from the μ-phenoxy-bridged manganese dimers would also allow an increase in the number of turnovers in the catalytic cycle. In turn, this would lead to the development of suitable catalysts from a technological perspective.

Experimental

Materials

All the starting materials (Aldrich) and solvents (Probus) used for the synthesis were of commercially available reagent grade and were used without further purification.

Physical measurements

Elemental analyses were performed on a Carlo Erba Model 1108 CHNS-O elemental analyser. The IR spectra were recorded as KBr pellets on a Bio-Rad FTS 135 spectrophotometer in the range 4000–400 cm^{-1}. ^1H spectra were recorded on a Bruker AC-300 spectrometer using DMSO-d_6 (296 K) as a solvent and $SiMe_4$ as an internal reference. FAB mass spectra were recorded on a Kratos MS50TC spectrometer connected to a DS90 data system, using *meta*-nitrobenzyl alcohol as a matrix. Room-temperature magnetic susceptibilities were measured using a digital measurement system MSB-MKI, calibrated using mercury tetrakis(isothiocyanato)cobaltate(II), $Hg[Co(NCS)_4]$, as a susceptibility standard. Electronic spectra were recorded on a Cary 230 spectrometer. Conductivities of 10^{-3} M solutions in DMF were measured on a Crison microCM 2200 conductivimeter. EPR measurements were carried out on a Bruker ESP300E X-band spectrometer equipped with an ER4116 DM dual-mode cavity and an Oxford 900 continuous flow cryostat. The typical temperature for EPR measurements was 9 K and other experimental conditions are shown in figure captions.

Electrochemical experiments (cyclic voltammetry, CV; and normal pulse voltammetry, NPV) were performed using an EG&G PAR model 273 potentiostat, controlled by EG&G PAR model 270 software. A Metrohm model 6.1204.000 graphite disc coupled to a Metrohm model 628–10 rotating electrolyte device was used as a working electrode. A saturated calomel electrode was used as a reference and a platinum wire used as an auxiliary electrode. All measurements were made with *ca.* 10^{-3} mol dm^{-3} solutions of the complexes in dimethylformamide using 0.2 mol dm^{-3} NBu_4PF_6 as a supporting electrode. Cyclic voltammetry measurements were performed with a static graphite electrode, whilst direct-current and pulse voltammograms were recorded with the graphite disc rotating at 2000 revolutions per minute.

Preparation of the Schiff base ligands

The asymmetrical Schiff bases were prepared in an analogous manner by the reaction of the appropriately substituted salicylaldehyde with diamine, and are typified by the following preparation.

To an ethanolic solution (100 mL) of 1,2-diamino-2,2-dimethylethane (0.83 mL, 7.8 mmol) was added 3OEt-salicylaldehyde (2.60 g, 15.60 mmol). The mixture was heated under reflux in a round-bottomed flask fitted with a Dean–Stark trap to remove the water produced during the reaction. After heating for 3 h, the solution was concentrated to yield a yellow solid. The product was collected by filtration, washed with diethyl ether and dried in air.

Yields were almost quantitative.

H_2L^1 (found: C, 68.8; H, 7.0; N, 7.1% calc. for $C_{22}H_{28}N_2O_4$ (384.47): C, 68.7; H, 7.3; N, 7.3%); ^1H NMR (300 MHz, [D_6]DMSO): δ = 13.70 (s, 2H), 8.53 (s, 1H), 8.50 (s, 1H), 6.69–7.00 (d, d, t, 6H), 4.00 (q, 4H), 3.96 (s, 2H), 1.34 (s, 6H), 1.30 (t, 6H) ppm. ES-MS: m/z = 385.4. IR ν(O–H) 3433 (m), ν(C=N) 1628 (*vs.*), ν(C–O) 1248 cm^{-1} (s); m. p. 88 °C.

H_2L^2 (found: C, 46.5; H, 4.5; N, 5.7% calc. for $C_{20}H_{22}Br_2N_2O_4$ (514.21): C, 46.7; H, 4.3; N, 5.4%); ^1H NMR δ = 1.42 (s, 6H), 3.72 (d, 2H), 3.88 (s, 6H), 6.9–7.3 (m, 4H), 8.21 (s, 1H), 8.23 (s, 1H), 13.80 (s, 1H), 14.45 (s, 1H); ES-MS: m/z = 515.1. IR ν(O–H) 3069 (m), ν(C=N) 1632 (*vs.*), ν(C–O) 1254 cm^{-1} (s); m. p. 133 °C.

H_2L^3 (found: C, 58.6; H, 5.2; N, 7.9% calc. for $C_{18}H_{18}Cl_2N_2O_2$ (365.26): C, 59.1; H, 5.0; N, 7.7%); ^1H NMR δ = 1.39 (s, 6H), 3.71 (d, 2H), 6.8–7.2 (m, 6H), 8.28 (s, 1H), 8.30 (s, 1H), 13.23 (s, 1H), 13.78 (s, 1H); ES-MS: m/z = 366.2. IR ν(O–H) 3063 (m), ν(C=N) 1634 (*vs.*), ν(C–O) 1260 cm^{-1} (s); m. p. 137 °C.

H_2L^4 (found: C, 49.2; H, 3.6; N, 6.4% calc. for $C_{18}H_{16}Cl_4N_2O_2$ (434.15): C, 49.8; H, 3.7; N, 6.4%); ^1H NMR δ = 1.46 (s, 6H), 3.80 (d, 2H), 7.1–7.4 (m, 4H), 8.17 (s, 1H), 8.20 (s, 1H), 14.05 (s, 1H), 14.82 (s, 1H); ES-MS: m/z = 425.2. IR ν(O–H) 3078 (m), ν(C=N) 1631 (*vs.*), ν(C–O) 1259 cm^{-1} (s); m. p. 150 °C.

Complex preparation

All of the complexes were synthesised by air oxidation of solutions of $Mn(ClO_4)_2{\cdot}6H_2O$ and the Schiff base.[60] A typical preparation is outlined below.

$[MnL^1(H_2O)_2]_2(ClO_4)_2$, **1**: H_2L^1 (1.56 mmol, 0.60 g) was dissolved in 1 : 1 methanol/ethanol (100 mL) and $Mn(ClO_4)_2{\cdot}6H_2O$ (1.56 mmol, 0.57 g) was added to the initial yellow solution, which changed to green (**CAUTION:** although problems were not encountered in this work, perchlorates are potentially explosive and should be handled in small quantities and with care!). The mixture was stirred for 10 min and NaOH (3.12 mmol, 0.13 g), dissolved in a small quantity of water, was added. The mixture became dark. The progress of the reaction was followed by TLC for 3 d and the mixture was then filtered. The complex was obtained from the filtrate as a brown solid after crystallisation. The solid was filtered off and washed with

diethyl ether and dried in air. Yield: 0.66 g (75%). Anal. calc. for $C_{44}H_{60}Cl_2Mn_2N_4O_{20}$ (1145.7): C, 46.1; H, 5.2; N, 4.9%. Found: C, 46.4; H, 5.1; N, 4.6%. MS FAB (*m*/*z*): 438 $[MnL]^+$; 875 $[Mn_2L_2]^+$. IR (KBr, cm^{-1}): ν(O–H) 3421 (m), ν(C=N) 1612 (*vs.*), ν(C–O) 1257 (s), $\nu(ClO_4^-)$ 1120 (*vs.*), 625 (m). μ = 5.0 BM. ^{1}H NMR (300 MHz, [D$_6$]DMSO): δ = −28.01 (H4), −17.16, −18.96 (H5) ppm. Conductivity (in DMF) Λ_M = 88 μS. E_{ox} = −0.092 V; E_{red} = −0.534 V; $E_{1/2}$ = −0.313 V.

$[MnL^2(H_2O)_2]_2(ClO_4)_2$, **2**, 1.94 mmol (1.00 g) of H_2L^2; 1.94 mmol (0.70 g) of $Mn(ClO_4)_2{\cdot}6H_2O$; 3.88 mmol (0.16 g) of NaOH; yield: 1.07 g (80%). Anal. calc. for $C_{40}H_{48}Br_4Cl_2Mn_2N_4O_{20}$ (1405.22): C, 34.2; H, 3.4; N, 4.0%. Found: C, 34.6; H, 3.2; N, 4.1%. MS FAB (*m*/*z*): 566 $[MnL]^+$; 1133 $[Mn_2L_2]^+$. IR (KBr, cm^{-1}): ν(O–H) 3421 (m), ν(C=N) 1626 (*vs.*), ν(C–O) 1262 (s), $\nu(ClO_4^-)$ 1120 (*vs.*), 625 (m). μ = 4.7 BM. ^{1}H NMR (300 MHz, [D$_6$]DMSO): δ = −27.82 (H4), −16.91, −18.70 (H5) ppm. Conductivity (in DMF) Λ_M = 78 μS. E_{ox} = −0.011 V; E_{red} = −0.414 V; $E_{1/2}$ = −0.213 V.

$[MnL^3(H_2O)_2]_2(ClO_4)_2$, **3**, 2.74 mmol (1.00 g) of H_2L^3; 2.74 mmol (0.99 g) of $Mn(ClO_4)_2{\cdot}6H_2O$; 5.48 mmol (0.22 g) of NaOH; yield: 0.91 g (60%). Anal. calc. for $C_{36}H_{40}Cl_6Mn_2N_4O_{16}$ (1107.3): C, 39.0; H, 3.6; N, 5.1%. Found: C, 39.8; H, 3.4; N, 5.3%. MS FAB (*m*/*z*): 419 $[MnL]^+$; 876 $[Mn_2L_2]^+$. IR (KBr, cm^{-1}): ν(O–H) 3421 (m), ν(C=N) 1616 (*vs.*), ν(C–O) 1268 (s), $\nu(ClO_4^-)$ 1121 (*vs.*), 625 (m). μ = 4.7 BM. ^{1}H NMR (300 MHz, [D$_6$]DMSO): δ = −28.30 (H4), −17.46, −18.85 (H5) ppm. Conductivity (in DMF) Λ_M = 93 μS. E_{ox} = 0.060 V; E_{red} = −0.325 V; $E_{1/2}$ = −0.133 V.

$MnL^4(H_2O)_2(ClO_4)$, **4**, 1.36 mmol (0.59 g) of H_2L^4; 1.36 mmol (0.49 g) of $Mn(ClO_4)_2{\cdot}6H_2O$; 2.72 mmol (0.11 g) of NaOH; yield: 0.61 g (75%). Anal. calc. for $C_{36}H_{40}Cl_{10}Mn_2N_4O_{18}$ (1281.1): C, 33.7; H, 3.1; N, 4.4%. Found: C, 34.5; H, 3.1; N, 4.2%. MS FAB (*m*/*z*): 487 $[MnL]^+$; 974 $[Mn_2L_2]^+$. IR (KBr, cm^{-1}): ν(O–H) 3421 (m), ν(C = N) 1622 (*vs.*), ν(C–O) 1268 (s), $\nu(ClO_4^-)$ 1118 (*vs.*), 625 (m). μ = 5.0 BM. ^{1}H NMR (300 MHz, [D$_6$]DMSO): δ = −28.15 (H4), −17.16, −18.81 (H5) ppm. Conductivity (in DMF) Λ_M = 84 μS. E_{ox} = 0.212 V; E_{red} = −0.178 V; $E_{1/2}$ = 0.017 V.

Crystallographic data collection and refinement of the structure

Single crystals of complex **1**, suitable for X-ray diffraction studies, were obtained by slow evaporation of the methanolic solution at room temperature.

Detailed crystal data collection and refinement are summarized in Table S1 (ESI‡). Intensity data were collected on a Bruker-Nonius KCCD2000 diffractometer using graphite-monochromated Cu-Kα radiation (λ = 1.54184 Å) for **1** at room temperature. The structure was solved by direct methods[61] and finally refined by a full-matrix least-squares base on F^2. An empirical absorption correction was applied using SADABS.[62] All non-hydrogen atoms were included in the model at geometrically calculated positions.

CCDC 821534 (for **1**) contains the supplementary crystallographic data for this paper.

Irradiation experiments

The irradiation of aqueous solutions of the manganese complexes was carried out in a colourless two-necked glass flask (1 L) placed in a methacrylate thermostatted water bath. A magnetically stirred solution of **1** (5×10^{-6} mol; 5.7 mg) and *p*-benzoquinone (2×10^{-4} mol; 21 mg) in deoxygenated and deionised water was irradiated with light (in the 350–2500 nm range) from a 200 W tungsten lamp for 24 h. The solution was connected to a UV spectrophotometer through a peristaltic pump and a flow cell. Quantitative measurements of the amount of dioxygen formed during irradiation were performed using a dissolved-oxygen probe-type electrode (Crison Oxi45P). The setting up of the experiment is depicted in Fig. S4 (ESI‡). In a typical experiment deionised deoxygenated water was placed in the two-necked glass flask: one neck contained the oxygen electrode and the second a septum. The whole flask arrangement was immersed in the thermostatted bath so that the water came up the base of the necks. Stirring was begun, the complex and quinone were added, and the septum fitted to make the system airtight. Four needles were pushed through the septum, one reaching into the liquid, and a stream of dinitrogen was introduced into the solution until the reading of the oxygen meter fell to <3%. Once this value was reached the N_2 needle and the purge needle were removed and the system was left stirring for 10 min to equilibrate. The light was switched on. Only the two needles connected to the flow cell remained through the septum. Oxygen readings were recorded as percentage dissolved oxygen where 100% corresponds to a fully saturated aqueous solution at 25 °C (6 cm^3 O_2 dm^{-3}) and 0% corresponds to no dissolved oxygen. Reproducible results were obtained with this method provided that the temperature of the bath remained constant (25.0 ± 0.1 °C) and a constant stirring rate was maintained.

Conclusions

The results obtained demonstrate the photogeneration of dioxygen from H_2O coordinated to manganese(III)-Schiff base μ-aqua dimers in the presence of *p*-benzoquinone. On the basis of a range of studies we propose that this reaction follows a mechanism involving successive hydrogen abstractions from water molecules coordinated to the metal ion by optically excited *p*-benzoquinone, and subsequent formation of a μ-phenoxy-bridged manganese(III) dimer.

Manganese(III)-Schiff base complexes were found to be active systems for water photolysis, although some questions remain about how they act. Further studies are necessary to address some of these questions in the search for more efficient catalysts.

Today we know that the structure of a Schiff base with essentially identical donor atoms can have a profound and often intriguing effect on the solid state and reactivity of the resultant complexes. Thus, novel synthetic systems should be tested. In our laboratories we are currently investigating the response to variations in the conductivity of the media, as well as the effect of changing the quinone and the use of bandpass filters through which the monitoring beam enters the sample solution in irradiation experiments. The use of these types of compounds as electrocatalysts for water oxidation is another planned research line. However, it would be extremely advantageous if scientists with diverse backgrounds set out to investigate, from the different perspectives of their own disciplines, the role and behaviour of these systems.

Acknowledgements

We thank Xunta de Galicia (09DPI004291PR) for financial support.

Notes and references

1 M. Yagi, A. Syouji, S. Yamada, M. Komi, H. Yamazaki and S. Tajima, *Photochem. Photobiol. Sci.*, 2009, **8**, 139–147.
2 A. Magnuson, M. Anderlund, O. Johansson, P. Lindblad, R. Lomoth, T. Polivka, S. Ott, K. Stensjö, S. Styring, V. Sundström and L. Hammarström, *Acc. Chem. Res.*, 2009, **42**, 1899–1909.
3 A. Inagaki and M. Akita, *Coord. Chem. Rev.*, 2010, **254**, 1220–1239.
4 J. McEvoy and G. Brudvig, *Chem. Rev.*, 2006, **106**, 4455–4483.
5 C. Cady, R. Crabtree and G. Brudvig, *Coord. Chem. Rev.*, 2008, **252**, 444–455.
6 F. Armstrong, *Philos. Trans. R. Soc. London, Ser. B*, 2008, **363**, 1263–1270.
7 M. Maneiro, W. F. Ruettinger, E. Bourles, G. L. McLendon and G. C. Dismukes, *Proc. Natl. Acad. Sci. U. S. A.*, 2003, **100**, 3707–3712.
8 S. Mukhopadhyay, S. Mandal, S. Bhaduri and W. Armstrong, *Chem. Rev.*, 2004, **104**, 3981–4026.
9 J. P. McEvoy and G. Brudvig, *Phys. Chem. Chem. Phys.*, 2004, **6**, 4754–4763.
10 J. Mayer, I. Rhile, F. Larsen, E. Mader, T. Markle and A. DiPasquale, *Photosynth. Res.*, 2006, **87**, 3–20.
11 C. Mullins and V. Pecoraro, *Coord. Chem. Rev.*, 2008, **252**, 416–443.
12 E. Sproviero, J. Gascon, J. McEvoy, G. Brudvig and V. Batista, *Coord. Chem. Rev.*, 2008, **252**, 395–415.
13 D. Pantazis, M. Orio, T. Petrenko, S. Zein, E. Bill and W. Lubitz, *Chem.–Eur. J.*, 2009, **15**, 5108–5123.
14 G. Dismukes, R. Brimblecombe, G. Felton, R. Pryadun, J. Sheats and L. Spiccia, *Acc. Chem. Res.*, 2009, **42**, 1935–1943.
15 M. Kanan and D. Nocera, *Science*, 2008, **321**, 1072–1075.
16 R. Brimblecombe, G. Dismukes, G. Swiegers and L. Spiccia, *Dalton Trans.*, 2009, 9374–9384.
17 M. Yagi, M. Toda, S. Yamada and H. Yamazaki, *Chem. Commun.*, 2010, **46**, 8594–8596.
18 H. Karunadasa, C. Chang and J. Long, *Nature*, 2010, **464**, 1329–1333.
19 P. Kurz, *Dalton Trans.*, 2009, 6103–6108.
20 M. Yagi, K. Narita, S. Maruyama, K. Sone, T. Kuwabara and K. Shimizu, *Biochim. Biophys. Acta, Bioenerg.*, 2007, **1767**, 660–665.
21 M. Collomb and A. Deronzier, *Eur. J. Inorg. Chem.*, 2009, 2025–2046.
22 H. Yamazaki, A. Shouji, M. Kajita and M. Yagi, *Coord. Chem. Rev.*, 2010, **254**, 2483–2491.
23 M. Calvin, *Science*, 1974, **184**, 375–381.
24 R. Ramaraj, A. Kira and M. Kaneko, *Chem. Lett.*, 1987, 261–264.
25 S. Cooper and M. Calvin, *Science*, 1974, **185**, 376.
26 J. Limburg, J. S. Vrettos, L. M. Liable-Sands, A. L. Rheingold, R. H. Crabtree and G. W. Brudvig, *Science*, 1999, **283**, 1524–1527.
27 A. Poulsen, A. Rompel and C. McKenzie, *Angew. Chem., Int. Ed.*, 2005, **44**, 6916–6920.
28 N. Aurangzeb, C. E. Hulme, C. A. McAuliffe, R. G. Pritchard, M. Watkinson, M. R. Bermejo, A. Garcia-Deibe, J. Sanmartin and A. Sousa, *J. Chem. Soc., Chem. Commun.*, 1994, 1153–1155.
29 F. Ashmawy, C. McAuliffe, R. Parish and J. Tames, *J. Chem. Soc., Dalton Trans.*, 1985, 1391–1397.
30 M. R. Bermejo, A. Castineiras, J. C. Garcia-Monteagudo, M. Rey, A. Sousa, M. Watkinson, C. A. McAuliffe, R. G. Pritchard and R. L. Beddoes, *J. Chem. Soc., Dalton Trans.*, 1996, 2935–2944.
31 M. R. Bermejo, M. I. Fernandez, A. M. Gonzalez-Noya, M. Maneiro, R. Pedrido, M. J. Rodriguez, J. C. Garcia-Monteagudo and B. Donnadieu, *J. Inorg. Biochem.*, 2006, **100**, 1470–1478.
32 M. Maneiro, M. R. Bermejo, M. Isabel Fernandez, E. Gomez-Forneas, A. M. Gonzalez-Noya and A. M. Tyryshkin, *New J. Chem.*, 2003, **27**, 727–733.
33 M. R. Bermejo, M. I. Fernandez, E. Gomez-Forneas, A. Gonzalez-Noya, M. Maneiro, R. Pedrido and M. J. Rodriguez, *Eur. J. Inorg. Chem.*, 2007, 3789–3797.
34 M. Maneiro, M. R. Bermejo, A. Sousa, M. Fondo, A. M. Gonzalez, A. Sousa-Pedrares and C. A. McAuliffe, *Polyhedron*, 2000, **19**, 47–54.
35 V. Daier, D. Moreno, C. Duhayon, J. Tuchagues and S. Signorella, *Eur. J. Inorg. Chem.*, 2010, 965–974.
36 M. Collomb, C. Mantel, S. Romain, C. Duboc, J. Lepretre and J. Pecaut, *Eur. J. Inorg. Chem.*, 2007, 3179–3187.
37 J. A. Bonadies, M. L. Maroney and V. L. Pecoraro, *Inorg. Chem.*, 1989, **28**, 2044–2051.
38 M. R. Bermejo, M. I. Fernandez, A. M. Gonzalez-Noya, M. Maneiro, R. Pedrido, M. J. Rodriguez and M. Vazquez, *Eur. J. Inorg. Chem.*, 2004, 2769–2774.
39 M. R. Bermejo, A. M. Gonzalez-Noya, V. Abad, M. I. Fernandez, M. Maneiro, R. Pedrido and M. Vazquez, *Eur. J. Inorg. Chem.*, 2004, 3696–3705.
40 M. R. Bermejo, A. G. Deibe, M. Rey, J. Sanmartin, A. Sousa, N. Aurangzeb, C. E. Hulme, C. A. McAuliffe and R. G. Pritchard, *J. Chem. Soc., Dalton Trans.*, 1994, 1265–1269.
41 E. Talsi and K. Bryliakov, *Mendeleev Commun.*, 2004, **14**, 111–112.
42 M. Maneiro, M. R. Bermejo, M. I. Fernandez, A. M. Gonzalez-Noya, A. M. Tyryshkin and R. G. Pritchard, *Z. Anorg. Allg. Chem.*, 2003, **629**, 285–290.
43 A. Ononye, A. McIntosh and J. Bolton, *J. Phys. Chem.*, 1986, **90**, 6266–6270.
44 P. Pospisil, D. Carsten and E. Jacobsen, *Chem.–Eur. J.*, 1996, **2**, 974–980.
45 W. J. Geary, *Coord. Chem. Rev.*, 1971, **7**, 81–122.
46 S. Lee, S. Chang, D. Kossakovski, H. Cox and J. Beauchamp, *J. Am. Chem. Soc.*, 1999, **121**, 10152–10156.
47 M. Awad and A. Anderson, *J. Am. Chem. Soc.*, 1989, **111**, 802–806.
48 M. Maneiro, M. R. Bermejo, M. Fondo, A. M. Gonzalez, J. Sanmartin, J. C. Garcia-Monteagudo, R. G. Pritchard and A. M. Tyryshkin, *Polyhedron*, 2001, **20**, 711–719.
49 R. C. Kapoor and B. S. Aggarwal, *Principles of polarography*, John Wiley, New York, 1991.
50 S. Hung, F. Yang, J. Chen, S. Wang and J. Tung, *Inorg. Chem.*, 2008, **47**, 7202–7206.
51 M. Horitani, H. Yashiro, M. Hagiwara and H. Hori, *J. Inorg. Biochem.*, 2008, **102**, 781–788.
52 C. Mantell, H. Chen, R. Crabtree, G. Brudvig, J. Pecaut and M. Collomb, *ChemPhysChem*, 2005, **6**, 541–546.
53 A. Abragam and B. Bleaney, *Electron paramagnetic resonance of transition ions*, Dover Publications, New York, 1986.
54 A. Barra, D. Gatteschi, R. Sessoli, G. Abbati, A. Cornia and A. Fabretti, *Angew. Chem., Int. Ed.*, 1997, **36**, 2329–2331.
55 H. Gerritsen and E. Sabisky, *Phys. Rev.*, 1963, **132**, 1507.
56 K. Campbell, D. Force, P. Nixon, F. Dole, B. Diner and R. Britt, *J. Am. Chem. Soc.*, 2000, **122**, 3754–3761.
57 G. Yin, A. Danby, D. Kitko, J. Carter, W. Scheper and D. Busch, *J. Am. Chem. Soc.*, 2008, **130**, 16245–16253.
58 M. Watkinson, M. Fondo, M. R. Bermejo, A. Sousa, C. A. McAuliffe, R. G. Pritchard, N. Jaiboon, N. Aurangzeb and M. Naeem, *J. Chem. Soc., Dalton Trans.*, 1999, 31–42.
59 K. Ghosh, A. Eroy-Reveles, M. Olmstead and P. Mascharak, *Inorg. Chem.*, 2005, **44**, 8469–8475.
60 L. Boucher and C. Coe, *Inorg. Chem.*, 1975, **14**, 1289–1295.
61 G. M. Sheldrick, *SHELX-97 (shelxs 97 and shelxl 97), Programs for Crystal Structure Analyses*, University of Göttingen, Germany, 1998.
62 G. M. Sheldrick, *SADABS, Program for Scaling and Correction of Area Detector Data*, University of Göttingen, Germany, 1996.